2022 44th Annual International Conference of
the IEEE Engineering in Medicine & Biology Society (EMBC)
Scottish Event Campus, Glasgow, UK, July 11-15, 2022

2022 44th Annual International Conference of the IEEE Engineering in Medicine & Biology Society (EMBC) | 978-1-7281-2782-8/22/$31.00 ©2022 IEEE | DOI: 10.1109/EMBC48229.2022.9871324

# A comparative study on recognizing human activities by applying diverse Machine Learning approaches

Lamprini G. Pappa, Petros Karvelis, and Chrysostomos D. Stylios, Senior Member, IEEE

*Abstract*— **This paper deals with the problem of identifying and recognizing everyday human activities. The main goal is to compare a variety of implemented classification models founded on diverse machine learning approaches; one that utilizes features extracted from the time and frequency domain and three others that take advantage of the attributes of the symbolic space in order to extract conclusions regarding the performance and the potential usefulness of each of them. To guarantee the impartiality of the comparison, we used the signals contained in a free accessible dataset, which are subjected to the same preprocessing, and divided into equal time-length windows. The Nearest Neighour classifier is applied to compare the four approaches.**

## I. Introduction

Nowadays, time-series data are generated and gathered at an unprecedented rate due to the general use of smartphones, sensors, RFID, and other devices [1], and in general, due to the rise and broad penetration of the Internet of Things in industry, business, medicine, and everyday life. There are many diverse applications such as medical data analysis, human activity recognition, and many others. Time-series data analysis assists in understanding system operation and improving our ability to gain insight, perception, and prediction of the evolution of various existences and states in the real world [2]. Usually, these data are always high-dimensional and have a high volume. Thus, researchers propose many dimensionality reduction methods to represent raw time series [3] effectively. Data representation in a lower-dimensional space provides a meaningful yet compact representation while maintaining the original, inherent information central to storing and mining these massive data [4]. Researchers have been developing many representation techniques for time series. The Symbolic Aggregate Approximation (SAX) by Lin et al. [5] is of particular interest. This technique segments a time series into intervals represented by their mean value, the so-called Piecewise Aggregate Approximation (PAA), and then it discretizes each mean value by mapping it to a discrete symbol. Nevertheless, the SAX method suffers from two significant drawbacks: first, two time series with totally different shapes may be mapped to the exact SAX representation, and secondly, it may lose some important features [2], [3].

Many variations of the SAX method have been implemented to deal with this innate defection of the SAX. We refer to the most recent. Entropy-based Symbolic Aggregate approXimation (EN_SAX) improves the original SAX by capturing an additional characteristic in a segment using the time series entropy [3]. Probabilistic SAX (pSAX) [4] is based on a Kernel Density Estimator (KDE) to estimate the density function of the data source, coupled with a Lloyd-Max quantizer for computing optimal discretization intervals. The clustering SAX (cSAX) [4] relies on the mean-shift clustering method to produce descriptive symbolic sequences, which are more appropriate for high-level data analysis tasks. Two recent variations of SAX that attempt to incorporate information related to the deterministic behavior of time series to increase the representation accuracy are sSAX and tSAX [6]. The former is aware of the season of a time series by assuming the existence of a seasonal component, while the latter is aware of the trend of a time series and captures this behavior in a trend component. Finally, HAX (Hexadecimal Aggregate approXimation) is a times series representation method to reduce its dimensionality and establish a similarity measure between two-time series objects [2]. In the current work, our objective is to test different machine learning approaches with emphasis on SAX variations that are already introduced in previous publications.

The rest of this paper is structured as follows. Section II describes the data set and the preprocessing stage. In section III, we describe the machine learning approaches we implemented. In section III.A, we explain the feature extraction approach, and the SAX method in section III.B. Next, in III.B.1) and III.B.2), we present two variations of SAX. In section IV, we demonstrate the comparative classification results. Furthermore, in section V, we draw some conclusions.

## II. DATA AND PREPROCESSING

We tested all the implemented machine learning approaches on the same dataset extracted from the publicly available web database, the RealWorld (HAR) [7]. We utilized the signals produced from the accelerometer and the device's gyroscope (a smartphone mounted on the subjects' body); that correspond to the triaxial linear acceleration and angular velocity. The subjects performed eight different activities for roughly 10 minutes. The activities are: climbing stairs down and up, jumping, lying, standing, sitting, running/jogging, and walking. The sampling rate was set at 50 Hz, while the amount of data was equally distributed regarding the subject's gender.

Before applying any machine learning approach, we first preprocess [8] the raw data of both the accelerometer and gyroscope, separately. Therefore, we applied filters to remove the unwanted noise: in sequence, a fifth-order median filter

Lamprini G. Pappa, Petros Karvelis, and Chrysostomos D. Stylios is with Laboratory of Knowledge and Intelligent Computing, University of Ioannina, Department of Informatics and Telecommunications, Arta, Greece.

and a fifth-order low-pass Butterworth filter with a 20 Hz cutoff frequency. Then we applied the z-score normalization (mean value of zero and standard deviation value equal to one). The processed signals can be compared; in other words, we can apply machine learning algorithms to remove the original signals' distortions. Finally, we segmented the filtered and z-normalized signals into sliding time windows of the same duration (2.56 sec) overlapped at 50% percentage.

After this step, we apply the machine learning algorithms in two different directions. We are experimenting with one supervised method based on feature extraction and another semi-supervised method based on the symbolic representation of time series.

## III. APPLIED MACHINE LEARNING APPROACHES

### *A. Feature Extraction*

Signals can be regarded as a time series, and corresponding measures can describe them. These measures stand for the features of a signal and represent the most distinct characteristics of a signal's nature. Features are obtained after transforming the signals or by statistically processing them. The selection of the best features (i.e., the most distinctive characteristics that provide valuable information to distinguish one signal from another) is crucial and relies much on the researcher's experience in understanding the nature of the undertaken problem. On the one hand, the selection of the best features aims to maximize the classification accuracy and, on the other hand, minimize the system's complexity.

The features most commonly used for human activity recognition problems fall into three sub-categories: those belonging to the time domain, those belonging to the frequency domain, and those combining the two fields mentioned above and derived after applying the Discrete Transformation Wavelet (Discrete Wavelet Transform - DWT). TABLE I presents the features that we used here alongside a short description of them. The reader can refer to the bibliography provided for more information [9]–[18].

TABLE I. THE LIST OF FEATURES EXTRACTED FROM THE TIME AND FREQUENCY DOMAIN

| No. | Feature | Meaning |
|---|---|---|
| 1 | min | The minimum amplitude value of a signal |
| 2 | max | The maximum amplitude value of a signal |
| 3 | mean | The mean amplitude value of a signal |
| 4 | bandpower | The average power within a frequency range of a signal |
| 5 | zero-crossing rate | The rate at which a signal changes from positive to negative and vice versa |
| 6 | variance | The averaged power of the signal's random deviations expressed as power [19] |
| 7 | kurtosis | The peakedness of the probability density function of the amplitude of a time series [20] |
| 8 | skewness | The symmetry of the probability density function of the amplitude of a time series [20] |
| 9 | root-mean-square | The square root of the mean square. It is related to the power of a signal |
| 10 | median frequency | The frequency at which the signal's power spectrum is divided into two regions with an equal integrated power [21] |
| 11 | entropy | A measure of the uncertainty of a random process |
| 12 | euclidean norm | The square root of a signal's energy |
| 13 | mean abs | The mean value of the absolute amplitude values of a signal |
| 14 | sum | The summing of all the amplitude values of a signal. |
| 15 | total power | The total power of all the frequencies of a signal |

We implemented a straightforward supervised machine learning algorithm, where every feature is computed in every time window that the signal is divided. Ultimately, we obtain the table of features of the implemented supervised machine learning method.

### *B. Symbolic Aggregate Approximation*

Lin et al. [5] introduced the SAX method to describe a procedure that enables the symbolic representation of time series. First of all, the dimensionality reduction of the problem is realised by applying the PAA technique [5], [22], [23]. The latter has direct positive implications in the speed and efficiency of an applied algorithm (complexity and time reduction are achieved). Then, we transform the real number space to symbolic space, where a variety of distance measures can be used (e.g., Euclidean, Manhattan, Minkowski) for comparing thse symbolic series.

All-in-all, the procedure is described in formula (1), where the dimensionality reduction and symbolic transformation phases are demonstrated.

$$X = \{x_1, x_2, \ldots, x_n\} \rightarrow X' = \{x_1', x_2', \ldots, x_m'\} \rightarrow S = \{s_1, s_2, \ldots, s_m\},\ m < n, \quad (1)$$

where $X$ is the processed time series of length $n$, $X'$ is the length-reduced time series of length $m$, $S$ is the corresponding symbolic series, and $x_i'$ is calculated by Equation (2).

$$x_i' = \frac{m}{n} \sum_{j=\frac{n}{m}(i-1)+1}^{\frac{n}{m}i} x_j \quad (2)$$

We highly recommend that the interested reader consult the step-by-step analysis described in [24] to understand the method thoroughly. The process is comprehensibly depicted in Figure 1.

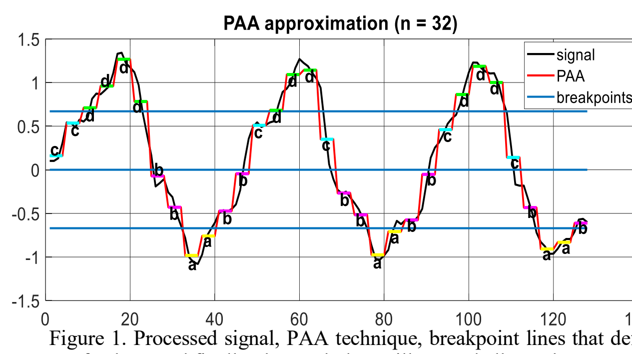


Figure 1. Processed signal, PAA technique, breakpoint lines that define ranges of values, and finally, the symbols are illustrated all together.

After extracting a symbolic series, we compute the so-called Intelligent Icons [25] that represent the frequency of occurrence of a group of symbols (called words) within a window having the meaning of a frequency distribution table. This table forms the table of features of this semi-supervised machine learning approach. Once again, it is recommended the reader refer to our past work [24].

### 1) Multichannel SAX Intelligent Icons

Multichannel SAX Intelligent Icons [24] is a variation of the Intelligent Icons that offers the omni-dimensional integration of information nested in every one-dimension symbolic series. Let us consider a three-dimensional signal (e.g., velocity). We apply the SAX method as described in III.B for each dimension, which results in obtaining three symbolic series. The differentiation from the formerly established Intelligent Icons extraction method is that we now search for groups of symbols (words) where each one of them comes from the corresponding symbolic series. Figure 2 coherently explains the procedure. Ultimately, we construct the frequency distribution table that refers to these words. The latter, alongside the table extracted in III.B, comprise the table of features of this approach.


Figure 2. Words consist of one symbol from every dimension for computing multichannel intelligent icon

### 2) Slopewise Aggregate Approximation SAX

The Slopewise Aggregate Approximation (SAA SAX) [26] is a variation of PAA. Instead of calculating the mean value of the values of datapoints in every segment, we calculate the mean value of the slopes of the lines formed by connecting every point to the first point of each segment. Consequently, the initial time series is transformed to angle values series, as is shown in formula (3).

$$X = \{x_1, x_2, \dots, x_n\} \rightarrow \Theta' = \{\theta_1{}', \theta_2{}', \dots, \theta_m{}'\}, m < n \quad (3)$$

where $\theta_i{}'$ is the average angle in every segment.

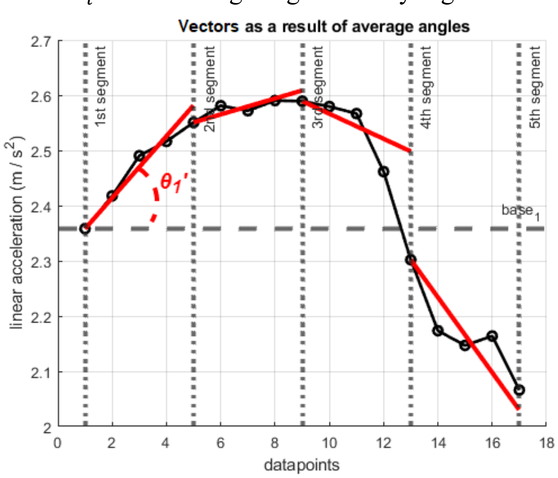


Figure 3. Every segment of the time series is replaced with a vector that has its initial point at the first point of the segment and forms an angle with the horizontal axis equal to $\theta_i{}'$. Red lines are the slope approximations, and the continuous black line is the signal.

This process has the advantage of avoiding losing useful information regarding the shape and fluctuation of the time series after the dimensionality reduction process. One can easily observe this fact by comparing Figure 1 and Figure 3. Figure 3 better describes the trend of the time series.

Then, we transform the values of the angles to symbols, and we extract the Intelligent Icons as in III.B. The latter, alongside the table extracted in III.B, comprise the table of features of this approach.

## IV. Results

Each one of the implemented approaches generates a different set of features. We randomly separate the initial dataset into a training dataset and a testing one. The training dataset includes the randomly extracted 80% of the features of every class, while the remaining 20% comprises the testing dataset. We employed a 1-Nearest Neighbour classifier to calculate each model's prediction accuracy and sensitivity. The execution of the Nearest Neighbour algorithm was repeated ten times in order for the results to be the least unbiased and prone to validation set's partialities. TABLE II depicts the average classification accuracy of the four models, whereas TABLE III displays the average values of the sensitivity, respectively. The results of the last three models are obtained from our past work [26]. Figure 4, graphically demonstrates the differences in the performance of each model regarding every activity to be recognised.

TABLE II. Comparative table between the four under-study Machine Learning approaches in terms of accuracy

| Accuracy (%) | | | |
|---|---|---|---|
| ***Feature extraction*** | ***SAX*** | ***Multichannel SAX*** | ***SAA SAX*** |
| 81.32 | 90.13 | 92.39 | 96.00 |

TABLE III. Comparative table between the four under-study Machine Learning approaches in terms of sensitivity

| **ACTIVITIES** | Sensitivity (%) | | | |
|---|---|---|---|---|
| | ***Feature extraction*** | ***SAX*** | ***Multichannel SAX*** | ***SAA SAX*** |
| Downstairs | 61.53 | 92.51 | 95.70 | 97.28 |
| Upstairs | 77.88 | 92.47 | 94.70 | 96.11 |
| Jumping | 65.63 | 95.89 | 96.89 | 96.76 |
| Lying | 91.58 | 89.92 | 92.10 | 96.81 |
| Running | 91.52 | 97.19 | 97.69 | 98.66 |
| Sitting | 82.42 | 80.20 | 83.87 | 92.66 |
| Standing | 80.65 | 81.62 | 85.13 | 92.20 |
| Walking | 81.28 | 96.11 | 97.22 | 98.15 |
| **MEAN VALUE** | **79.06** | **90.74** | **92.91** | **96.08** |

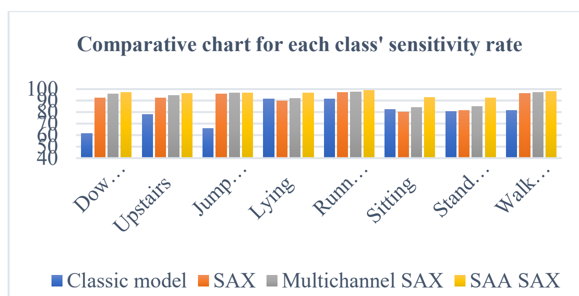


Figure 4. Bar chart indicating the performance of each developed machine learning model in terms of each class' sensitivity rates.

The first model exhibits the poorest results in terms of efficiency. On the contrary, the implementations based on symbolic representations demonstrate a significantly high classification rate. Regarding specific activities, it is noteworthy to refer to "Downstairs" and "Jumping," where an increase of thirty percentage units is met with the symbolic representations. "Upstairs" performance also seems to be considerably boosted by the latter.

On the other hand, SAA SAX seems to improve the recognition performance for all the activities, even for those presenting a somewhat moderate performance among the other two symbolic representations approaches.

## V. Conclusion

In the current study, we focused on comparing the performance of four classification models using the same dataset as a benchmark for rendering our work impartial, and simultaneously all the parameters defining the model were set at the same value. Our goal was to indicate the usefulness and merit of working with the symbolic representation of time series. Our intention was not to search for the optimal performance using the best classifier but rather to test the different approaches using the same classifier.

There are some innate weaknesses regarding such implementations, such as the need to define parameters; therefore, there is a need to investigate the optimum parameters' values. However, these methods' advantages make their further study and experimenting on them worth it

## Acknowledgment

This research work is funded by the Operational Programme "Epirus" 2014-2020, under the project "Integrated Support System for elderly people with health problems and lonely workers using Portable Devices and Machine learning Algorithms – TrackMyHealth", Co-financed by the European Regional Development Fund (ERDF).

## References

[1] Z. He and X. Ma, "A Distributed Indexing Method for Timeline Similarity Query," Algorithms, vol. 11, no. 4, Art. no. 4, Apr. 2018, doi: 10.3390/a11040041.

[2] Z. He, C. Zhang, X. Ma, and G. Liu, "Hexadecimal Aggregate Approximation Representation and Classification of Time Series Data," Algorithms, vol. 14, no. 12, Art. no. 12, Dec. 2021, doi: 10.3390/a14120353.

[3] H. Zhang, Y. Dong, and D. Xu, "Entropy-based Symbolic Aggregate Approximation Representation Method for Time Series," in 2020 IEEE 9th Joint International Information Technology and Artificial Intelligence Conference (ITAIC), Dec. 2020, vol. 9, pp. 905–909. doi: 10.1109/ITAIC49862.2020.9339021.

[4] K. Bountrogiannis, G. Tzagkarakis, and P. Tsakalides, "Distribution Agnostic Symbolic Representations for Time Series Dimensionality Reduction and Online Anomaly Detection," arXiv:2105.09592 [cs], May 2021, Accessed: Jan. 03, 2022. [Online]. Available: http://arxiv.org/abs/2105.09592

[5] J. Lin, E. Keogh, S. Lonardi, and B. Chiu, "A symbolic representation of time series, with implications for streaming algorithms," in Proceedings of the 8th ACM SIGMOD workshop on Research issues in data mining and knowledge discovery, New York, NY, USA, Jun. 2003, pp. 2–11. doi: 10.1145/882082.882086.

[6] L. Kegel, C. Hartmann, M. Thiele, and W. Lehner, "Season- and Trend-aware Symbolic Approximation for Accurate and Efficient Time Series Matching," Datenbank Spektrum, vol. 21, no. 3, pp. 225–236, Aug. 2021, doi: 10.1007/s13222-021-00389-5.

[7] T. Sztyler and H. Stuckenschmidt, "On-body localization of wearable devices: An investigation of position-aware activity recognition," in 2016 IEEE International Conference on Pervasive Computing and Communications (PerCom), Sydney, Australia, Mar. 2016, pp. 1–9. doi: 10.1109/PERCOM.2016.7456521.

[8] J. G. Proakis and D. G. Manolakis, Digital signal processing, 4th ed. Upper Saddle River, N.J: Pearson Prentice Hall, 2007.

[9] A. L. G. N. Gomes, "Human Activity Recognition with Accelerometry: Novel Time and Frequency Features," p. 127, 2014.

[10] Ç. B. Erdaş, I. Atasoy, K. Açıcı, and H. Oğul, "Integrating Features for Accelerometer-based Activity Recognition," Procedia Computer Science, vol. 98, pp. 522–527, Jan. 2016, doi: 10.1016/j.procs.2016.09.070.

[11] L. Cao, Y. Wang, Q. Jin, and J. Ma, "ActiRecognizer: Design and Implementation of a Real-Time Human Activity Recognition System," in 2017 International Conference on Cyber-Enabled Distributed Computing and Knowledge Discovery (CyberC), Oct. 2017, pp. 266–271. doi: 10.1109/CyberC.2017.71.

[12] S. Rosati, G. Balestra, and M. Knaflitz, "Comparison of Different Sets of Features for Human Activity Recognition by Wearable Sensors," Sensors, vol. 18, no. 12, Art. no. 12, Dec. 2018, doi: 10.3390/s18124189.

[13] S. J. Preece, J. Y. Goulermas, L. P. J. Kenney, D. Howard, K. Meijer, and R. Crompton, "Activity identification using body-mounted sensors--a review of classification techniques," Physiol Meas, vol. 30, no. 4, pp. R1-33, Apr. 2009, doi: 10.1088/0967-3334/30/4/R01.

[14] L. Bao and S. S. Intille, "Activity Recognition from User-Annotated Acceleration Data," in Pervasive Computing, Berlin, Heidelberg, 2004, pp. 1–17. doi: 10.1007/978-3-540-24646-6_1.

[15] A. Bulling, U. Blanke, and B. Schiele, "A tutorial on human activity recognition using body-worn inertial sensors," ACM Comput. Surv., vol. 46, no. 3, p. 33:1-33:33, Jan. 2014, doi: 10.1145/2499621.

[16] M. Zhang and A. A. Sawchuk, "A feature selection-based framework for human activity recognition using wearable multimodal sensors," in Proceedings of the 6th International Conference on Body Area Networks, Brussels, BEL, Nov. 2011, pp. 92–98.

[17] M. H. M. Noor, Z. Salcic, and K. I.-K. Wang, "Adaptive sliding window segmentation for physical activity recognition using a single tri-axial accelerometer," Pervasive and Mobile Computing, vol. 38, pp. 41–59, Jul. 2017, doi: 10.1016/j.pmcj.2016.09.009.

[18] L. Gao, A. K. Bourke, and J. Nelson, "Evaluation of accelerometer based multi-sensor versus single-sensor activity recognition systems," Medical Engineering & Physics, vol. 36, no. 6, pp. 779–785, Jun. 2014, doi: 10.1016/j.medengphy.2014.02.012.

[19] "Average Deviation, Standard Deviation, and Variance in Signal Processing - Technical Articles." https://www.allaboutcircuits.com/technical-articles/average-deviation-standard-deviation-variance-signal-processing/ (accessed Dec. 29, 2021).

[20] "Understanding Basic Statistical Values (Advanced Signal Processing Toolkit) - LabVIEW 2010 Advanced Signal Processing Toolkit Help - National Instruments." https://zone.ni.com/reference/en-XX/help/371419D-01/lvasptconcepts/tsa_basic_stat_analysis/ (accessed Dec. 29, 2021).

[21] S. Thongpanja, A. Phinyomark, P. Phukpattaranont, and C. Limsakul, "Mean and Median Frequency of EMG Signal to Determine Muscle Force based on Time-Dependent Power Spectrum," ElAEE, vol. 19, no. 3, pp. 51–56, Mar. 2013, doi: 10.5755/j01.eee.19.3.3697.

[22] E. Keogh, K. Chakrabarti, M. Pazzani, and S. Mehrotra, "Dimensionality Reduction for Fast Similarity Search in Large Time Series Databases," Knowledge and Information Systems, vol. 3, no. 3, pp. 263–286, Aug. 2001, doi: 10.1007/PL00011669.

[23] J. Lin, E. Keogh, L. Wei, and S. Lonardi, "Experiencing SAX: a novel symbolic representation of time series," Data Min Knowl Disc, vol. 15, no. 2, pp. 107–144, Oct. 2007, doi: 10.1007/s10618-007-0064-z.

[24] L. Pappa, P. Karvelis, G. Georgoulas, and C. Stylios, "Multichannel Symbolic Aggregate Approximation Intelligent Icons: Application for Activity Recognition," in 2020 IEEE Symposium Series on Computational Intelligence (SSCI), Dec. 2020, pp. 505–512. doi: 10.1109/SSCI47803.2020.9308497.

[25] E. Keogh, L. Wei, X. Xi, S. Lonardi, J. Shieh, and S. Sirowy, "Intelligent Icons: Integrating Lite-Weight Data Mining and Visualization into GUI Operating Systems," in Sixth International Conference on Data Mining (ICDM'06), Dec. 2006, pp. 912–916. doi: 10.1109/ICDM.2006.90.

[26] L. Pappa, P. Karvelis, G. Georgoulas and C. Stylios, "Slopewise Aggregate Approximation SAX: keeping the trend of a time series," 2021 IEEE Symposium Series on Computational Intelligence (SSCI), 2021, pp. 01-08, doi: 10.1109/SSCI50451.2021.9660130.